ZrO₂ Nanoparticles: Optical Properties of Tetragonal Phase and Enhanced Photocatalytic Activity

Hana Aminipoya[1], Azar Bagheri Ghomi[*,1], Saeed Rayati[2]

[1] Department of Chemistry, Central Tehran Branch, Islamic Azad University, Tehran, Iran

[2] Department of Chemistry, K. N. Toosi University of Technology, Tehran P. O. Box 16315-1618, Iran

Abstract: Tetragonal zirconia (t-ZrO2) nanoparticles were synthesized from the zirconium chloride using the co-precipitation technique and characterized by various measurement techniques. FESEM analysis further revealed spherical shaped NPs and HR-TEM analysis determined the size of the particles in the range of 14.5 nm. The band gap energy was estimated 4.0 eV. The UV (350 nm) emission was observed from PL spectrum. The photocatalytic degradation of the as-prepared ZrO2 nanoparticles were studied under UV light irradiation using ciprofloxacin (CIP) as a model organic pollutant. Results showed that 50% degradation were achieved within 15 min.

Keywords: ZrO₂, Photoluminescence, Tetragonal Phase, Band Gap, Photocatalytic Activity

1. INTRODUCTION

Nanometric ZrO2 particles are a technologically important class of materials with a wide range of applications [1]. Pure zirconia can exist in three crystallographic forms, cubic, tetragonal and monoclinic. The ZrO₂ band gap in the monoclinic, tetragonal and ZrO2 cubes are in the range of 3.12-5.42, 4.10-13.30 and 3.25-12.30, respectively [2]. The electronic configuration of the ions is the reason for this difference. It is well known that morphological amendment, porosity, crystallinity, and bandgap plays a major role in light absorption ability, separation of photogenerated charge carriers and the accessibility to surface active sites to participate photocatalytic reaction. Hence, in the present report, we report the synthesis of tetragonal ZrO2 (t-ZrO2) nanoparticles using co-precipitation technique. The metallic ZrO2 nanoparticles

∗ Corresponding author. Email: **Azar.bagheri@iauctb.ac.ir**

have been received significant attention because of their various potential applications [3], and also plays a significant role in photocatalysis research because of their high surface to volume ratio [4-6].The photogenerated charge carriers have high redox ability due to its wide band gap property. Zheng et al. synthesized ZrO2 nanocrystals using L-Lysine and studied the photocatalytic activity using Rh B as model pollutant with 63.39 % efficiency in 5h [7]. Therefore, we made an attempt to enhance the photocatalytic activity of pure t-ZrO2 nanoparticles under UV light through the modification of precursor materials and synthesis procedure. ZrO2 nanoparticles have been synthesized by various techniques [8-15]. Few of the reported methods require costly equipment, difficult processes and high production cost that result in a complex process and specific control. We present a new rout for synthesis of pure tetragonal ZrO2 with high crystalinity, using a rapid, simple and cost-effective chemical method.

2. EXPERIMENTAL

2.1 MATERIAL
Zirconium chloride (99.9% Sigma Co.) and ethanol (99.9% Sigma Co.) were used as received, without further purification. Other compounds used were prepared from MERCK company

2.2.APPARATUS
Phase identification of the fabricated sample was carried out by an Holland Philips X-ray diffraction CuKα (λ=1.5417 Å) in the radiation range of 20°–80°. A Field emission scanning electron micrograph (FeSEM) of a Holland Philips XL30 microscope was used to observe the morphology and elemental analysis of the sample. The Raman spectrum was recorded in the spectral range 200–1400 cm^{-1} using Almega Thermo Nicolet Raman spectrometer. The presence of surface functional groups in the prepared samples was analyzed by FTIR spectrum recorded using Perkin Elmer FTIR spectrometer. Spectrophotometric measurements were conducted using an UV-VIS Shimadzu 2101 spectrophotometer equipped with a Acermate 486 SX/25D computer and thermostically matched 10-mm quartz cells.

2.3 SYNTHESIS OF ZrO2
3.3 *m*mol KOH was dissolved in 36 ml distilled water under stirring. Then 3 mmol the template, hexamethylenetetramine, was added to the solution. Zirconium chloride (3 mmol) was added to the mixture. The mixture was refluxed for 4 h in 110 ℃. ZrO2 was obtained by centrifugation and drying of precipitate at room temperature. Then the ZrO2 nanoparticle was obtained via controlled calcination process using muffle furnace for 3hrs at 600 ℃.

3. RESULTS AND DISCUSSION

3.1. STRUCTURAL ANALYSIS

Fig. 1 provides a typical XRD pattern of product obtained from co-precipitation method in an aqueous solution. In Fig. 1, where the major (111) peak of tetragonal ZrO2 is identified. Using the full width at half-maximum intensity (FWHM) of the (111) peak, Fig. 1, obtained via narrow scan analysis and using the Scherer Eq the average tetragonal nanodomain size of 14 nm is calculated [16]. The obtained average crystallite size from TEM is 14.5 nm (Fig.2). The smaller size of crystallite indicates the existence of oxygen vacancies at the surface and at grain boundaries. The presence of oxygen vacancies will prevent the nanoparticles growth and produce a stress field. The produced defects will act as a scattering center for electron, hole and stimulate the recombination of the electron– hole pairs which influencing the photocatalytic activity and photoluminescence performance.
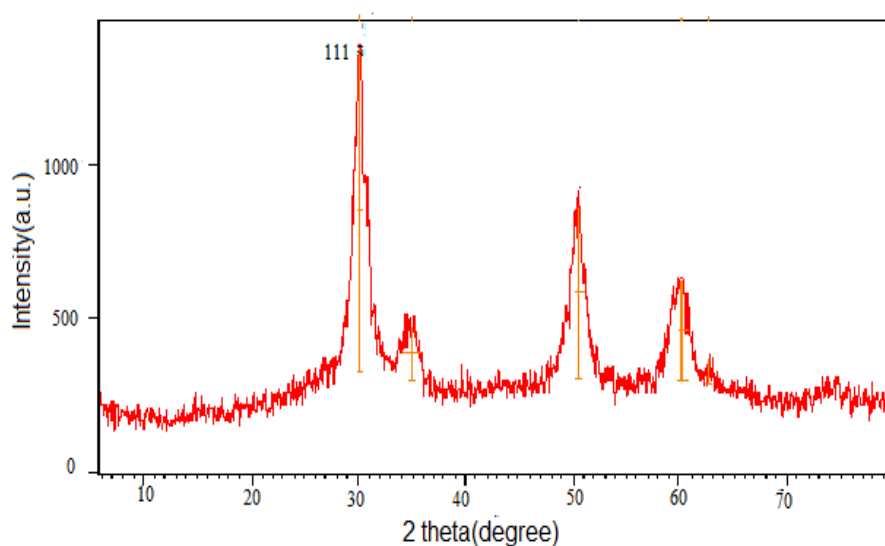
Fig.1: XRD pattern of the synthesized ZrO_2 nanoparticles
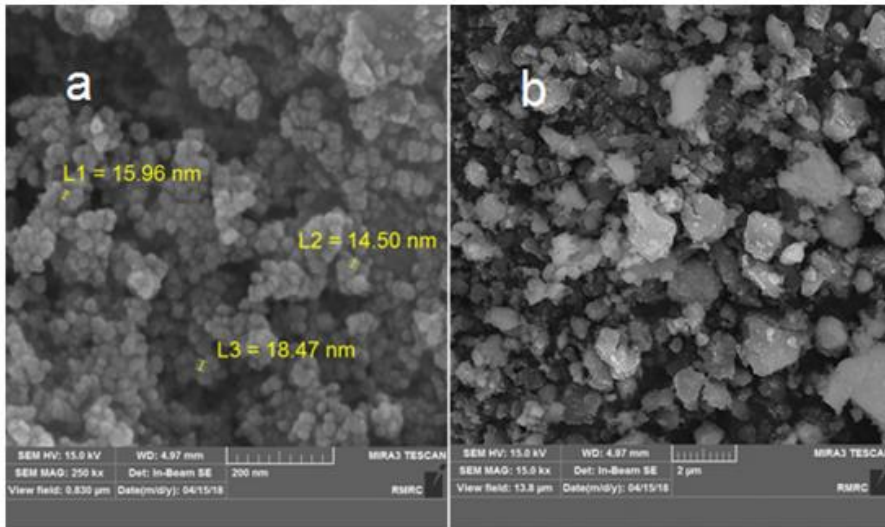
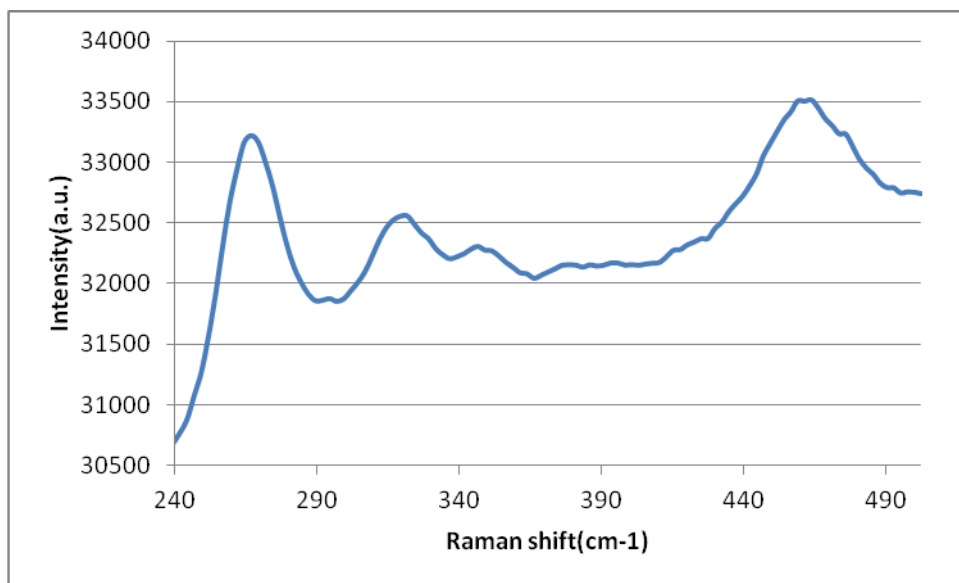**Fig.2:** FE-SEM image of the synthesized ZrO_2 nanoparticles
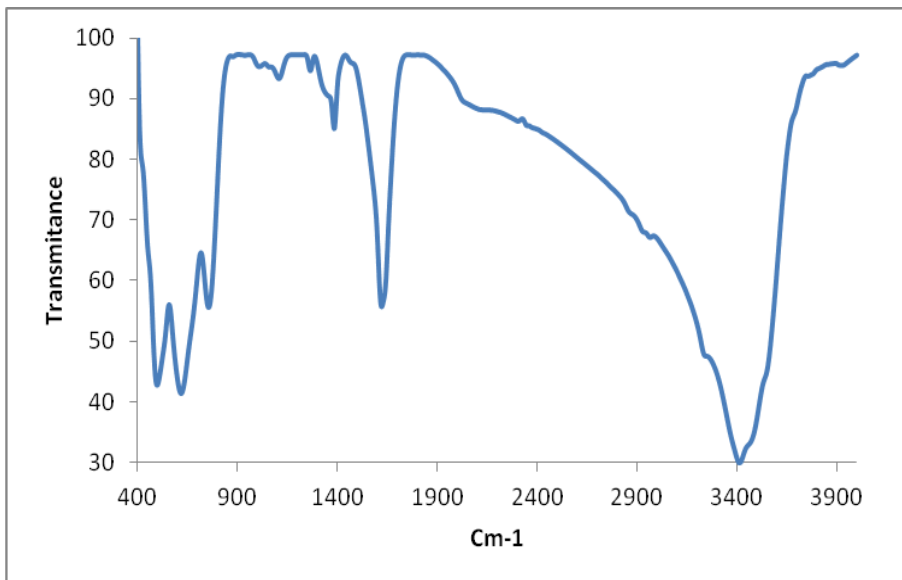
Fig.3:FT-IR spectra of synthesized ZrO_2 nanoparticles

Spectrum of ZrO_2 NPs had shown peaks at 3412 cm^{-1} due to OH stretching, at 1620 cm-1 because of OH bending and at 492.73 cm-1 denoting Zr-O band, respectively. A band identified at 754 cm^{-1} is corresponding to m-ZrO_2, as per previously mentioned in the Raman analysis Based on the fingerprint characters of the peak positions, shapes and intensities along with the essential components in the materials were observed.

The intensity of peaks directly gave an idea about the amount of the groups present in the sample. A higher amount of surface hydroxyl groups over ZrO_2 showed high potential in the photocatalytic activity.

3.3. RAMAN ANALYSIS

Raman spectroscopy which has been extensively used to discriminate different structures of ZrO_2. Fig. 4 shows the Raman spectra of ZrO_2 NPs. As per group theory, the phases for monoclinic 18(9Ag+9Bg), tetragonal 6(1A_{1g}+ 2B_{1g}+ 3 Eg) and cubic 3(T_{2g}) crystalline phases are expected [17]. The vibrational Raman active modes for the t- ZrO2 crystalline phase are given as: $\Gamma = A_{1g} + 2B_{1g} + 3$ Eg. In general, the oxygen atoms only transfer in the z-direction in the A1g mode. In the B_{1g} mode, atom motion also in the zdirection, but Zr and O both contribute in this mode. In the Eg mode, Zr and O atoms pass in the x–y plane [18]. Since Zirconia has low phonon energy, Raman active lattice phonons were expected in spectral region 100-550 cm-1. The Raman bands at 147 and 260 cm-1 (Eg and B1g) confirms the presence of tetragonal phase [19].

**Fig. 4:** Raman spectra of ZrO_2 nanoparticles with method of co-precipitation
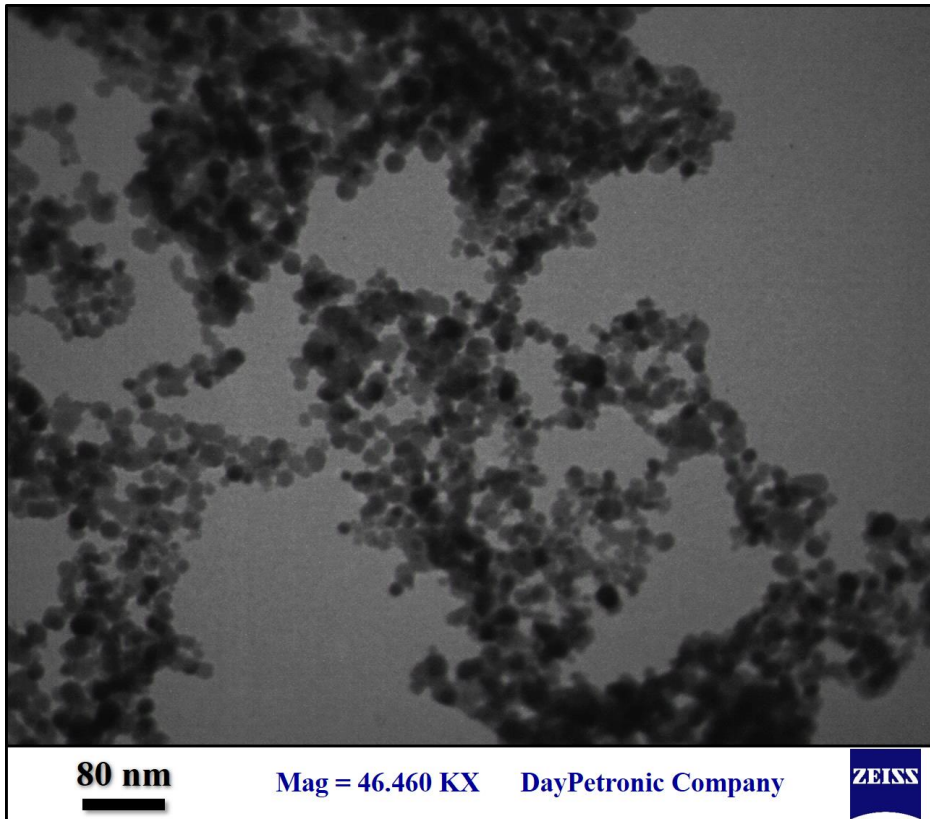
Fig.5: HR-TEM image of the synthesized ZrO2

HR-TEM image of ZrO2 nanoparticles is shown in Fig. 5 and it indicates the existence of well-organized lattices fringe of ZrO2. The fringe arrangements inside the crystallite show the development of a single phase ZrO2 with an extended order in the crystallite structure. The HR-TEM image shows the presence of aggregated spherical and tetragonal shaped NPs with average particle size of 15 nm.

3.4 PHOTOLUMINESCENCE AND OPTICAL ABSORPTION STUDIES
Photoluminescence (PL) technique can be used to study the migration, transfer and recombination rate of photogenerated electron–hole pairs in the semiconductor. In general, pure ZrO2 shows various emission of a broadband that is dependent on preparation methods and wavelength excitation [20]. Fig. 6(a) shows the photoluminescence (PL) spectrum of ZrO2 nanoparticles excited at 350 nm.
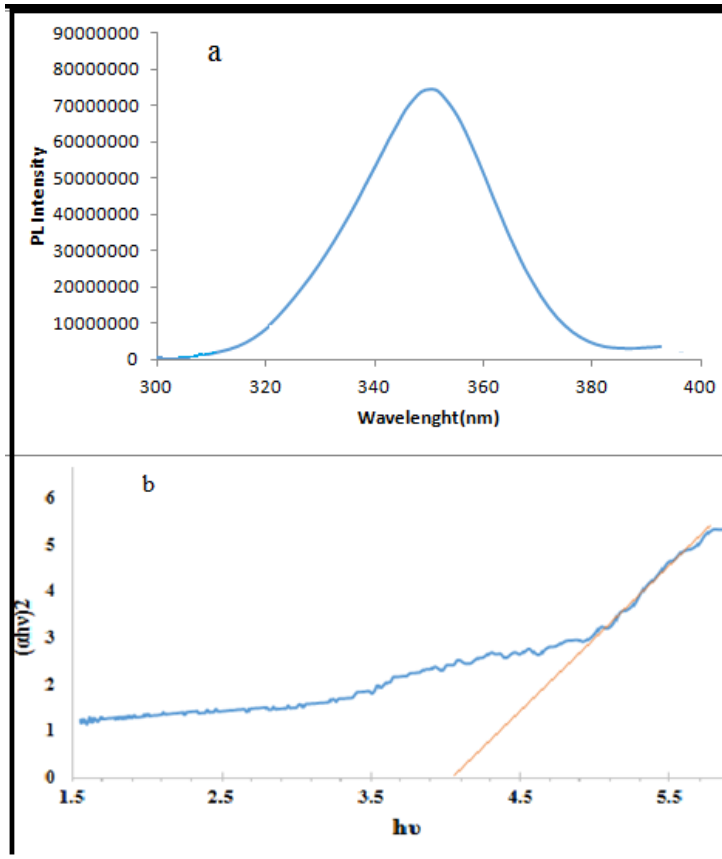
Fig. 6: (a) Photoluminescence spectrum of ZrO2 nanoparticles, b) Plot of (αhv)2 versus energy of the light absorbed of the ZrO2 nanoparticles

The peak observed at 350 nm corresponds to the ionized oxygen vacancies from the conduction band to the valence band [21, 22]. In this study, the surface defects increases on the synthesized ZrO2 nanoparticles that due to its high surface area. Similar results are reported in the literature for t-ZrO2 systems [23,24].

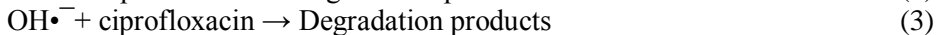Band gap energy of the loaded samples was estimated by Kubelka–Munk function using Eq(1):

$$\alpha = \frac{A\left(E_g - h\nu\right)^n}{h\nu}$$

(1)

Where E_g is the band gap of the proposed semiconductor (eV), A is constant and n is equal to1/2 for direct transition, and ، α is the absorption coefficient defined by the Beer–Lambert's law. The plot of $(\alpha h\nu)^2$ Vs hν of ZrO_2 is shown in Fig. 6b.

The size reduction in the nanoparticle can cause the change in optical band gap of metal oxides over the narrowing of the valence and conduction bands. The valance band of ZrO2 is mainly composed of occupied 2p energy state of O atom and the conduction band is constituted by unoccupied energy state 4d (x2-y2, z2) of Zr atom. Moreover, the optical band gap can affects defect centers, and mechanical stress. The direct optical band gap energy can be evaluated by using the relation 1. The obtained direct band gap value of ZrO2 nanoparticles is found to be 4.0 eV (Fig. 6b). The obtained value is in good agreement with values reported in the literature [25,4].

3.5. PHOTOCATALYTIC ACTIVITY

The photocatalytic activity of the ZrO2 nanoparticles were studied for the degradation of ciprofloxacin (CIP) under ultra violet (UV) light. Fig. 7 shows the optical absorption spectra of CIP using ZrO2 nanoparticles as a photocatalyst under UV light radiation. The absorption spectrum of the drug shows two strong peak at 277 nm and 320 nm. As seen in the figure, the decomposition of the drug increases with increasing irradiation time. When UV light is irradiated on the photocatalyst (t-ZrO2) material, electrons excited to conduction band from valence band. Produced electrons and holes are trapped by oxygen vacancies on the surface and water (H2O) molecules to create superoxide radicals ($O2^-\bullet$) and hydroxyl radicals ($OH\bullet^-$), respectively. Finally, the generated radicals interact with the pollutant to degrade it effectively.

$$O2^-\bullet + \text{ciprofloxacin} \rightarrow \text{Degradation products} \qquad (2)$$
$$OH\bullet^- + \text{ciprofloxacin} \rightarrow \text{Degradation products} \qquad (3)$$

The surface hydroxyl groups of ZrO2 are acidic and the amount of degradation enhances under acidic conditions. From the XRD analysis, it is clear that the prepared sample has the high crystallinity material, which supposed to be advantageous for photocatalysis because of the amount of defect sites in the structure. The photocatalytic activity of ZrO2 nanooxides for CIP degradation efficiency reaches 50% after 15 min.
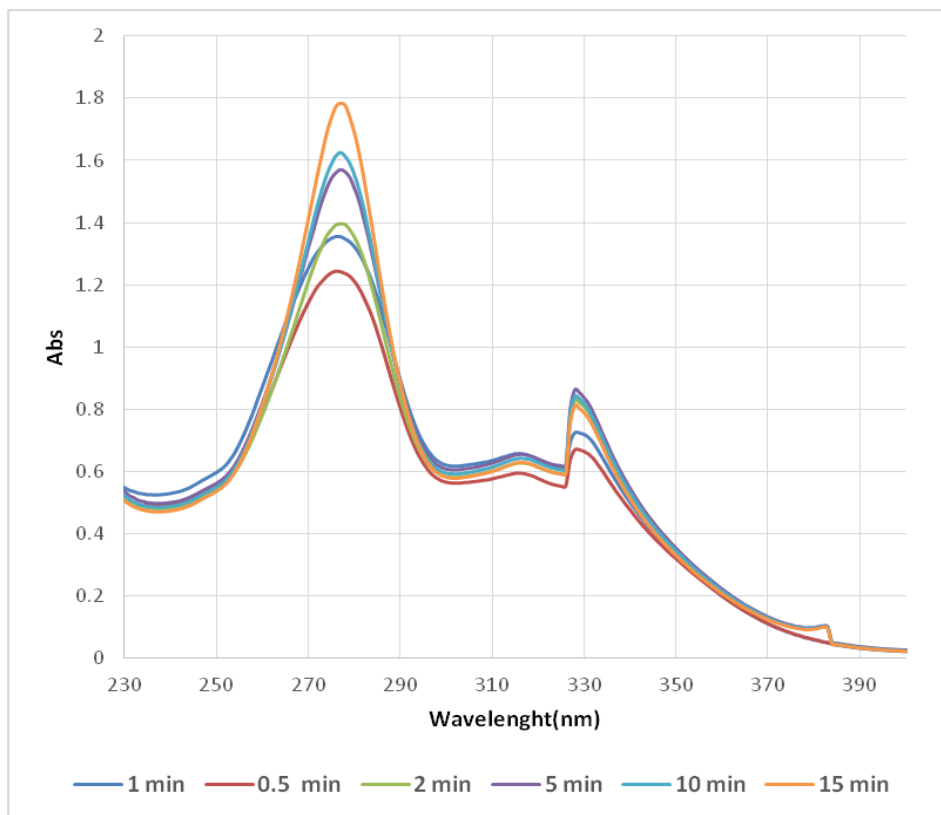
Fig.7 : Decrease in the UV–vis absorption of CIP at its λmax during the photod egradation

4. CONCLUSION

In this present report, t-ZrO2 nanoparticles were successfully synthesized using a simple method. The tetragonal crystal structure was confirmed by X-ray diffraction patterns. The average crystallite size was evaluated by XRD and HRTEM measurements techniques. The observed Raman bands at 350 and 700 cm^{-1} are characteristic of tetragonal crystal phase. The CIP degradation was achieved 50% within 15 min. During this time, the CIP solution will adsorb active facets of ZrO2. Since the freely obtainable charge carriers take part in the catalytic activity and very minute degradation is observed. When UV light is irradiated on the photocatalyst (t-ZrO2) material, electrons excited to conduction band from valence band. Furthermore, the same number of holes creates in the valence band. The photocatalytic activity is mainly ascribed due to

the high crystallinity, number of oxygen vacancies, larger surface area, larger pore volume and reduction in band gap energy due to less crystallite size.

REFERENCES

[1] (a) J. Si, S. B. Desu, C. Y. J. Tsai, *Metal-organic chemical vapor deposition of ZrO2 films using Zr(thd)4 as precursors* Mater. Res. 9 (7) (1994)1721.

[2] Sue-min Chang , Ruey-an Doong, *Interband transition of sol-gel-derived ZrO2 films under different calcination conditions*, Chemistry of Materials, 19(2007)4804-4810

[3] C. Wang, Y. Li, B. Cheng, *Fabrication of porous ZrO2 hollow sphere and its adsorption performance to Congo red in water*Ceram. Intr. 40 (2014) 10847-10856.

Metal-organic chemical vapor deposition of ZrO2 films using Zr(thd)4 as precursors

[4] F. Davar, M. R. Loghman-Estarki, *Synthesis and optical properties of pure monoclinic zirconia nanosheets by a new precursor*, Ceram. Int. 40 (2014) 8427–8433.

[5] L. Renuka, K.S. Anantharaju, S.C. Sharma, H. Nagabhushana, Y.S. Vidya, H.P.Nagaswarupa, S.C. Prashantha, *A comparative study on the structural, optical,electrochemical and photocatalytic properties of ZrO2 nanooxide synthesized by different Routes*, J. Alloy. Compound. 695 (2017) 382-395

[6] T.Razegh; V. Setoodeh; S. Pilban Jahromi *Influence of particle size on magnetic behavior of nickel oxide nanoparticles,J.Optoelect.Nanostruct.* 2(2017) 11-18

[7] H. Zheng, K. Liu, H. Cao, X. Zhang, *L-Lysine-Assisted Synthesis of ZrO2 Nanocrystals and Their Application in Photocatalysis*, J. Phys. Chem. C. 113 (2009) 18259–18263.

[8] D. Vollath, K.E. Sickafus, *Synthesis of nanosized ceramic oxide powders by microwave plasma reactions*, Nanostruct. Mater. 1 (1992) 427-437.

[9] W. S. Lee, S. W. Kim, B. H. Koo, D. S. Bae, *Synthesis and microstructure of Y2O3-doped ZrO2–CeO2 composite nanoparticles by hydrothermal process*, Colloids and Surfaces A: Physicochem. Eng. Aspects 313–314 (2008) 100–104

[10] N.L. Wu, T.F. Wu, *Enhanced Phase Stability for Tetragonal Zirconia in Precipitation Synthesis,* J. Am. Ceram. Soc. 83 (2000) 3225-3227.

[11] Sh. Ahmad Khan, Zh. Fu, S. Shakir Rehman, Muhammad Asif,WeiminWang, Hao Wang, *Study of template-free synthesis*

hierarchical m-ZrO2 nanorods by hydrothermal method, Powder Technology 256 (2014) 71–74.

[12] C.Y. Tai, B.Y. Hsiao, *characterization of zirconia powder synthesized via reversemicro emulsion precipitation*, Chem. Eng. Commun. 192 (2005) 1525-1540.

[13] T. Razpotnik, J. Macek, *Synthesis of nickel oxide/zirconia powders via a modified Pechini method,* J. Eur. Ceram. Soc. 27 (2007) 1405-1410.

[14] Cihangir Duran, KimiyasuSato, YujiHotta, HasanGöçmez, Koji Watari, *Ball milling assisted hydrothermal synthesis of ZrO2 nanopowders*, Ceram. Int, 41 (2015) 5588–5593.

[15] M. Gateshki, V. Petkov, G. Williams, S.K. Pradhan, Y. Ren, *Atomic-scale structure of nanocrystalline ZrO2 prepared by high-energy ball milling* Phys. Rev. B 71 (2005) 224107.

[16] Cullity, B. D. *Elements of X-ray Diffraction*; Addison-Wesley: Reading, MA, 1978

[17] K.A. Singh, L.C.Pathak, S.K.Roy, *Effect of citric acid on the synthesis of nanocrystalline yttria stabilized zirconia powders by nitrate-citrate process*, Ceram. Int. 33(2007)1463–1468.

[18] A. P. Naumenko, N. I. Berezovska, M. M. Biliyand, O.V. Shevchenko, *VibrationalAnalysis and Raman Spectra of Tetragonal Zirconia*, J. Mater. Sci. Lett. 9 (2008) 121–125

[19] G. Ehrhart, M. Bouazaoui, B. Capoen, V. Ferreiro, R. Mahiou, O. Robbe, S. Turrell, *Effects of rare-earth concentration and heat-treatment on the structural and luminescence properties of europium-doped zirconia sol–gel planar waveguides* Opt.Mater. 29 (2007)1723-1730

[20] K. Smits, L. Grigorjeva, D. Millers, A. Sarakovskis, J. Grabis, W. Lojkowski, *Intrinsic defect related luminescence in ZrO2*, J. Lumin. 131 (2011) 2058-2062.

[21] Sachin Kumar, Snehasis Bhunia, Jitendra Singh, Animesh K. Ojha, *Absence of room temperature ferromagnetism in Fe stabilized ZrO2 nanostructures and effect of Fe doping on its structural, optical and luminescence properties,* J. Alloy. Compound. 649 (2015) 348 - 356

[22] Christoph Reimann, Thomas Bredow, *Adsorption of nitrogen and ammonia at zirconia surfaces*, J. Mol. Struct. (THEOCHEM) 903 (2009) 89-99

[23] J. Liang, Z. Deng, X. Jiang, F. Li, and Y. Li, *Photoluminescence of tetragonal ZrO2 nanoparticles synthesized by microwave irradiation*, Inorg. Chem. 41 (2002) 3602–3604.

[24] Reena Dwivedi, Anjali Maurya, Akrati Verma, R. Prasad, K.S. Bartwal, *Microwave assisted sol–gel synthesis of tetragonal zirconia nanoparticles,* J. Alloy. Compound. 509 (2011) 6848–6851.

[25] M. Angeles-Rosas, M. A. *Camacho-López, E. Ruiz-Trejo, Structure, conductivity and luminescence of 8 mol% Scandia doped zirconia prepared by sol–gel,* Solid State Ion,181(2010)1349–1354.